

Quantum phase transition in a minimal model for the Kondo effect in a Josephson junction

Akira OGURI, Yoshihide TANAKA, and A. C. HEWSON¹

Department of Material Science, Osaka City University, Sumiyoshi-ku, Osaka 558-8585, Japan

¹*Department of Mathematics, Imperial College, 180 Queen's Gate, London SW7 2BZ, UK*

(Received June 12, 2004)

We propose a minimal model for the Josephson current through a quantum dot in a Kondo regime. We start with the model that consists of an Anderson impurity connected to two superconducting (SC) leads with the gaps $\Delta_\alpha = |\Delta_\alpha| e^{i\theta_\alpha}$, where $\alpha = L, R$ for the lead at left and right. We show that, when one of the SC gaps is much larger than the others $|\Delta_L| \gg |\Delta_R|$, the starting model can be mapped exactly onto the single-channel model, which consists of the right lead of Δ_R and the Anderson impurity with an extra onsite SC gap of $\Delta_d \equiv \Gamma_L e^{i\theta_L}$. Here θ_L and Γ_L are defined with respect to the starting model, and Γ_L is the level width due to the coupling with the left lead. Based on this simplified model, we study the ground-state properties for the asymmetric gap, $|\Delta_L| \gg |\Delta_R|$, using the numerical renormalization group (NRG) method. The results show that the phase difference of the SC gaps $\phi \equiv \theta_R - \theta_L$, which induces the Josephson current, disturbs the screening of the local moment to destabilize the singlet ground state typical of the Kondo system. It can also drive the quantum phase transition to a magnetic doublet ground state, and at the critical point the Josephson current shows a discontinuous change. The asymmetry of the two SC gaps causes a re-entrant magnetic phase, in which the in-gap bound state lies close to the Fermi level.

KEYWORDS: Kondo effect, Josephson effect, quantum phase transition, Anderson model, numerical renormalization group, quantum dot

1. Introduction

The Kondo effect in superconducting (SC) materials was originally studied for dilute magnetic alloys.¹⁻³ In normal metals, the ground state of the magnetic impurity is known to be a spin singlet, as a result of the antiferromagnetic coupling with the conduction electrons.⁴ However, in the presence of the SC long-range order, the energy gap of the host material disturbs the conduction electron screening of the local moment of the magnetic impurities. It was shown in early years that whether the local moment is screened or not is determined by the ratio of the Kondo temperature T_K to the SC gap Δ . The ground state becomes a doublet for $\Delta \gg T_K$, but it is still a singlet for $\Delta \ll T_K$. In contrast to the normal metals, for which the magnetic solution of the mean-field theory⁵ does not describe the correct ground state, in the superconducting case the bound state appearing in the energy gap causes the occurrence of a quantum phase transition to a magnetic doublet ground state.

These aspects of the Kondo physics in superconductors have been re-examined precisely by efficient numerical methods such as the quantum Monte Carlo (QMC)⁶ and Wilson numerical renormalization group (NRG) approaches.⁷⁻¹⁰ Furthermore, it has also been reconsidered for novel systems such as quantum dots.^{11,12} One of the new features in the quantum dot coupled to two SC leads is that the ground-state properties of the system can be controlled by the phase difference of the two SC gaps ϕ . It induces the Josephson current flowing through the dot, and at the same time it affects the screening of the local moment. When the local moment remains unscreened, the spin-flip tunnelling through the magnetic

impurity causes a current flowing in the opposite direction to that in the case of the normal junctions. An explanation has been given based on the lowest-order perturbation theory with respect to the spin-flip tunnelling Hamiltonian or equivalently treating the magnetic moment to be a classical spin.¹³⁻¹⁵ However, in the Kondo regime, the quantum-mechanical nature of the moment is essential to the screening. Therefore, in order to clarify how the Josephson current and the dynamics of the moment affect each other, the higher order terms in the tunnelling matrix element must be taken into account. So far, several studies have been carried out using the non-crossing approximation (NCA),^{16,17} slave-boson mean-field (SBMF) theory,^{18,19} perturbation theory in U ,²⁰ QMC,²¹ and NRG.²² Rozhkov and Arovas compared the ground-state energy for $\phi = 0$ and $\phi = \pi$ to discuss the phase transition from the 0 to π phase.¹⁸ Clerk and Ambegaoka pointed out that this transition can be explained in terms of the bound state appearing in the SC gap,¹⁷ as in the case of the magnetic impurity in the bulk superconductors.¹⁻³ So far, mainly one special case, in which the absolute value of the two SC gaps are the same $|\Delta_L| = |\Delta_R|$ and the couplings to the two leads are equal $\Gamma_L = \Gamma_R$, has been examined.^{16-20,22} However, the asymmetry in the two gaps $|\Delta_L| \neq |\Delta_R|$ and that in the mixing parameters $\Gamma_L \neq \Gamma_R$ affect sensitively the SC proximity effects on the impurity site. The superconducting correlations penetrating from the two leads determine the effective field that is coupled directly to the impurity. Therefore, the asymmetries in the gaps and in the mixing matrix elements, as well as the phase difference ϕ , will also affect the bound state and low-temperature proper-

ties of the impurity.

The purpose of this work is to study the interplay of the Josephson current and the dynamics of the local moment. To this end, we start with the Anderson impurity that is connected to two SC leads. Although it is already a simplified model, it still contains a number of parameters. In the present paper we mainly consider the asymmetric gap of $|\Delta_L| \gg |\Delta_R|$, where one of the SC gaps is much larger than the others. We show that in the limit of $|\Delta_L| \rightarrow \infty$ the starting model can be mapped onto a single-channel model, in which the left lead is chopped off leaving an extra onsite SC gap of $\Delta_d \equiv \Gamma_L e^{i\theta_L}$ at the impurity site. This single-channel model possesses both the Josephson and Kondo aspects since the phase difference can be defined with respect to Δ_d and Δ_R , and the simplification gives us a great advantage in carrying out numerical calculations. Based on this single-channel model, we examine the ground-state properties for $|\Delta_L| \gg |\Delta_R|$ using the NRG method. The phase diagram of the ground state is calculated for a wide parameter range of the Coulomb interaction U and the mixing strength Γ_R . The results show that the phase difference ϕ tends to make the stability of the singlet ground state worse, and it can hold a casting vote to determine whether the ground state is a singlet or doublet when the other parameters are competing. Specifically, at $\phi \simeq \pi$, $\Gamma_L \simeq \Gamma_R$, and near half-filling, the bound state lies close to the Fermi level, and it causes a re-entrant behavior of the magnetic doublet ground state.

In §2, the starting model and the mapping onto the single-channel model are described. In §3, the bound state in the noninteracting case is discussed briefly. In §4 the results of NRG calculations are presented. Summary is given in §5. In Appendix, the perturbation theory for a zero-energy bound state and other related matters are provided.

2. Mapping onto a single-channel Model

In this section we introduce the single-channel model, which captures the essence of both the Josephson and Kondo physics, starting from the model consisting of a single impurity and two SC leads.

The Hamiltonian of the Anderson impurity connected to two superconducting leads, at left (L) and right (R), is given by

$$\mathcal{H} \equiv \mathcal{H}_d^0 + \mathcal{H}_d^U + \sum_{\lambda=L,R} (\mathcal{H}_\lambda + \mathcal{H}_{d\lambda}^T), \quad (1)$$

where \mathcal{H}_d^0 and \mathcal{H}_d^U represent the impurity part, and $\lambda = L, R$ is the label assigned for the SC leads. The explicit form of each part is given by

$$\mathcal{H}_d^0 = \left(\epsilon_d + \frac{U}{2} \right) (n_d - 1), \quad \mathcal{H}_d^U = \frac{U}{2} (n_d - 1)^2, \quad (2)$$

$$\begin{aligned} \mathcal{H}_\lambda &= \sum_{k\sigma} \epsilon_{\lambda k} c_{\lambda k\sigma}^\dagger c_{\lambda k\sigma} \\ &+ \sum_k \left(\Delta_\lambda c_{\lambda k\uparrow}^\dagger c_{\lambda -k\downarrow}^\dagger + \Delta_\lambda^* c_{\lambda -k\downarrow} c_{\lambda k\uparrow} \right), \quad (3) \end{aligned}$$

$$\mathcal{H}_{d\lambda}^T = - \sum_\sigma v_\lambda \left(c_{\lambda\sigma}^\dagger d_\sigma + d_\sigma^\dagger c_{\lambda\sigma} \right). \quad (4)$$

The operator d_σ^\dagger creates an electron with spin σ at the dot, and $n_d = \sum_\sigma d_\sigma^\dagger d_\sigma$. Similarly, $c_{\lambda k\sigma}^\dagger$ creates a conduction electron in the lead at λ , and $\epsilon_{\lambda k}$ and Δ_λ are the energy and SC gap for the electrons in the lead, respectively. The tunnelling Hamiltonian $\mathcal{H}_{d\lambda}^T$ connects the dot at the center and lead at λ . At the interface the local operator of the conduction electrons is defined by $c_{\lambda\sigma} = \sum_k c_{\lambda k\sigma} / \sqrt{N}$. Correspondingly, the current flowing into the dot from the left lead J_L , and the current flowing out to the right lead J_R , are given by

$$J_L = iev_L \sum_\sigma \left(d_\sigma^\dagger c_{L\sigma} - c_{L\sigma}^\dagger d_\sigma \right), \quad (5)$$

$$J_R = iev_R \sum_\sigma \left(c_{R\sigma}^\dagger d_\sigma - d_\sigma^\dagger c_{R\sigma} \right). \quad (6)$$

Note that we are using units $\hbar = 1$ unless otherwise noted.

To discuss the superconducting properties, we use 2×2 matrix Green's function of the Nambu formulation,

$$\mathbf{G}_{dd}(\tau) = - \begin{bmatrix} \langle T_\tau d_\uparrow(\tau) d_\uparrow^\dagger \rangle & \langle T_\tau d_\uparrow(\tau) d_\downarrow \rangle \\ \langle T_\tau d_\downarrow^\dagger(\tau) d_\uparrow^\dagger \rangle & \langle T_\tau d_\downarrow^\dagger(\tau) d_\downarrow \rangle \end{bmatrix}. \quad (7)$$

The Fourier transform of the impurity Green's function, $\mathbf{G}_{dd}(i\omega_n) = \int_0^\beta d\tau e^{i\omega_n \tau} \mathbf{G}_{dd}(\tau)$, can be expressed as

$$\begin{aligned} \{\mathbf{G}_{dd}(i\omega_n)\}^{-1} &= i\omega_n \mathbf{1} - E_d \boldsymbol{\tau}_3 - v_L^2 \boldsymbol{\tau}_3 \mathbf{g}_L(i\omega_n) \boldsymbol{\tau}_3 \\ &- v_R^2 \boldsymbol{\tau}_3 \mathbf{g}_R(i\omega_n) \boldsymbol{\tau}_3 - \boldsymbol{\Sigma}(i\omega_n), \quad (8) \end{aligned}$$

where $E_d \equiv \epsilon_d + U/2$, and $\boldsymbol{\tau}_i$ for $i = 1, 2, 3$ is the Pauli Matrix, and $\boldsymbol{\Sigma}(i\omega_n)$ is the self-energy due to \mathcal{H}_d^U . Also, the Green's function for the bulk superconductor is given by $\{\mathbf{g}_{\lambda k}(i\omega_n)\}^{-1} = i\omega_n \mathbf{1} - \epsilon_{\lambda k} \boldsymbol{\tau}_3 - \Delta_\lambda$. The interface Green's function which enters in Eq. (8) is defined by $\mathbf{g}_\lambda(i\omega_n) \equiv \sum_k \mathbf{g}_{\lambda k}(i\omega_n)/N$, and can be written as

$$\mathbf{g}_\lambda(i\omega_n) = -\pi \rho_\lambda(0) \frac{i\omega_n \mathbf{1} + \Delta_\lambda}{\sqrt{\omega_n^2 + |\Delta_\lambda|^2}}, \quad (9)$$

where the density of states $\rho_\lambda(\epsilon) = \sum_k \delta(\epsilon - \epsilon_{\lambda k})/N$ has been assumed to be a constant. The SC order parameter enters in the off-diagonal element of Δ_λ ,

$$\Delta_\lambda \equiv \begin{bmatrix} 0 & \Delta_\lambda \\ \Delta_\lambda^* & 0 \end{bmatrix} = |\Delta_\lambda| (\cos \theta_\lambda \boldsymbol{\tau}_1 - \sin \theta_\lambda \boldsymbol{\tau}_2), \quad (10)$$

where $\Delta_\lambda = |\Delta_\lambda| e^{i\theta_\lambda}$. When the phase difference $\phi \equiv \theta_R - \theta_L$ is finite, the Josephson current flows through the impurity. Furthermore, due to the hybridization with the electrons in the SC leads, the superconducting correlation $\chi_d \equiv \langle d_\downarrow d_\uparrow \rangle$, which corresponds to the off-diagonal element of \mathbf{G}_{dd} , evolves at the impurity site.

In the noninteracting case, $\mathcal{H}_d^U = 0$, the impurity Green's function is given by

$$\begin{aligned} \{\mathbf{G}_{dd}^0(i\omega_n)\}^{-1} &= \\ i\omega_n \mathbf{1} - E_d \boldsymbol{\tau}_3 + \Gamma_L \frac{i\omega_n \mathbf{1} - \Delta_L}{\sqrt{\omega_n^2 + |\Delta_L|^2}} + \Gamma_R \frac{i\omega_n \mathbf{1} - \Delta_R}{\sqrt{\omega_n^2 + |\Delta_R|^2}}, \quad (11) \end{aligned}$$

where $\Gamma_\lambda = \pi \rho_\lambda(0) v_\lambda^2$. Correspondingly, the onsite SC correlation and Josephson current can be written as

$$\chi_d^0 = \frac{1}{\beta} \sum_{\omega_n} \frac{1}{\det \{ \mathbf{G}_{dd}^0(i\omega_n) \}^{-1}} \times \left[\frac{\Gamma_L \Delta_L}{\sqrt{\omega_n^2 + |\Delta_L|^2}} + \frac{\Gamma_R \Delta_R}{\sqrt{\omega_n^2 + |\Delta_R|^2}} \right], \quad (12)$$

$$\langle J_R \rangle^0 = \frac{e}{\beta} \sum_{\omega_n} \frac{-1}{\det \{ \mathbf{G}_{dd}^0(i\omega_n) \}^{-1}} \times \frac{4 \Gamma_R \Gamma_L |\Delta_R| |\Delta_L| \sin(\theta_R - \theta_L)}{\sqrt{\omega_n^2 + |\Delta_R|^2} \sqrt{\omega_n^2 + |\Delta_L|^2}}, \quad (13)$$

where $\beta = 1/T$, and $\langle J_L \rangle^0 = \langle J_R \rangle^0$. The Coulomb interaction U disturbs the SC correlation to penetrate into the impurity. This tendency can be seen already in an approximation of the Hartree-Fock level, through an anomalous contribution^{2,9}

$$\mathcal{H}_d^U \simeq U \left[d_{\uparrow}^\dagger d_{\downarrow}^\dagger \langle d_{\downarrow} d_{\uparrow} \rangle + \langle d_{\uparrow}^\dagger d_{\downarrow}^\dagger \rangle d_{\downarrow} d_{\uparrow} \right] + \dots \quad (14)$$

This term corresponds to a Fock term in the Nambu formulation

$$\Sigma_F = U \begin{bmatrix} 0 & \chi_d \\ \chi_d^* & 0 \end{bmatrix}, \quad (15)$$

and has a different sign from that of the attractive interaction which drives the leads superconducting states. However, to study precisely the effects of the Coulomb interaction on the Josephson current and on the SC correlations at the impurity, the higher-order terms beyond the mean-field theory should be taken into account. To carry out nonperturbative calculations, the present version of Anderson impurity already contains a number of parameters compared to that in the normal leads, i.e., we have $|\Delta_\lambda|$ and θ_λ in addition to Γ_λ , ϵ_d and U . Therefore, it seems to be meaningful to examine some special cases, at which the model can be simplified without losing the essence of Josephson and Kondo physics. In the following, we consider some such special cases.

2.1 Model I: $|\Delta_L| = |\Delta_R|$

One of the cases that has been studied by a number of authors so far is $|\Delta_L| = |\Delta_R|$ ($\equiv \Delta$), where the absolute value of the two gaps are equal. Physically, it means that the two leads are made of the same SC material. In this case the noninteracting Green's function can be written in the form

$$\{ \mathbf{G}_{dd}^0(i\omega_n) \}^{-1} = i\omega_n \mathbf{1} - E_d \boldsymbol{\tau}_3 + (\Gamma_L + \Gamma_R) \frac{i\omega_n \mathbf{1} - \tilde{\Delta}}{\sqrt{\omega_n^2 + \Delta^2}}, \quad (16)$$

$$\tilde{\Delta} \equiv \frac{\Delta}{\Gamma_L + \Gamma_R} \left[(\Gamma_L \cos \theta_L + \Gamma_R \cos \theta_R) \boldsymbol{\tau}_1 - (\Gamma_L \sin \theta_L + \Gamma_R \sin \theta_R) \boldsymbol{\tau}_2 \right], \quad (17)$$

and thus we have only one characteristic energy scale for the superconductivity, i.e., Δ . However, in this case the two-channel nature of the system is still preserved for finite ϕ . This feature can be seen in the functional

form of $\mathbf{G}_{dd}^0(i\omega_n)$ in Eq. (16). It becomes equivalent to that of a single-channel model only for $e^{i\theta_R} = e^{i\theta_L}$, when the amplitude of $\tilde{\Delta}$ coincides with Δ , i.e., $\tilde{\Delta}^2 = \Delta^2 \mathbf{1}$. Therefore, in the case of $|\Delta_L| = |\Delta_R|$, both of the superconductors must be taken into account explicitly to investigate the Josephson effect.

2.2 Model II: $|\Delta_L| \gg |\Delta_R|$

The situation is different when one of the gaps is much larger than the other's, $|\Delta_L| \gg |\Delta_R|$. Specifically, in the limit of $|\Delta_L| \rightarrow \infty$, the noninteracting Green's function $\mathbf{G}_{dd}^0(i\omega_n)$ can be written as

$$\{ \mathbf{G}_{dd}^0(i\omega_n) \}^{-1} = i\omega_n \mathbf{1} - E_d \boldsymbol{\tau}_3 - \Gamma_L \boldsymbol{\tau}_1 - v_R^2 \boldsymbol{\tau}_3 \mathbf{g}_R(i\omega_n) \boldsymbol{\tau}_3. \quad (18)$$

where the phase of Δ_L is chosen to be $\theta_L = 0$. One notable feature is that the third term in the right-hand side of Eq. (18) can be regarded as a static superconducting gap induced at the impurity site, and its value is given by Γ_L . This term comes from the mixing self-energy due the left lead $v_L^2 \boldsymbol{\tau}_3 \mathbf{g}_L(i\omega_n) \boldsymbol{\tau}_3$, and in the limit of $|\Delta_L| \rightarrow \infty$ the off-diagonal SC correlation remains finite to penetrate into the impurity site while the diagonal damping part corresponding to the level width vanishes. Therefore, in the case of $|\Delta_L| \gg |\Delta_R|$ the information about the left lead can be included through the off-diagonal $\Gamma_L \boldsymbol{\tau}_1$ term of the impurity Green's function, which can also be described by an effective single-channel Hamiltonian with an extra SC gap at the impurity site $\Delta_d \equiv \Gamma_L$,

$$\mathcal{H}_{\text{eff}} \equiv \mathcal{H}_d^0 + \mathcal{H}_d^U + \mathcal{H}_d^{\text{SC}} + \mathcal{H}_R + \mathcal{H}_{dR}^T, \quad (19)$$

$$\mathcal{H}_d^{\text{SC}} = \Delta_d \left[d_{\uparrow}^\dagger d_{\downarrow}^\dagger + d_{\downarrow} d_{\uparrow} \right]. \quad (20)$$

The phase difference ϕ defined with respect to the starting model is described by the phase difference between Δ_R and Δ_d . Using the effective Hamiltonian \mathcal{H}_{eff} , one can calculate the expectation values such as the Josephson current $\langle J_R \rangle$ and the Green's function $\mathbf{G}_{dd}(i\omega_n)$ for the interacting electrons, which coincide with that of the starting model in the limit of $|\Delta_L| \rightarrow \infty$. The mapping introduced here is exact. It can be confirmed, for instance, using the path integral formulation: the same effective action for the impurity can be derived from both \mathcal{H} and \mathcal{H}_{eff} after carrying out the integration over the conduction-electron degrees of freedom [see Appendix A]. The single-channel Hamiltonian \mathcal{H}_{eff} can be regarded as a minimal model that possesses both the Josephson and Kondo aspects of the system. This simplification gives us a great advantage in carrying out numerical calculations. Particularly, the NRG approach works excellently for single-channel systems, while the numerical accuracy becomes rather worse for multi-channel systems because the number of the low-lying states that should be retained in the calculation increases with the number of the channels. Therefore, in the present study, we mainly consider the asymmetric SC gap of $|\Delta_L| \gg |\Delta_R|$ using the single-channel Hamiltonian Eq. (19).

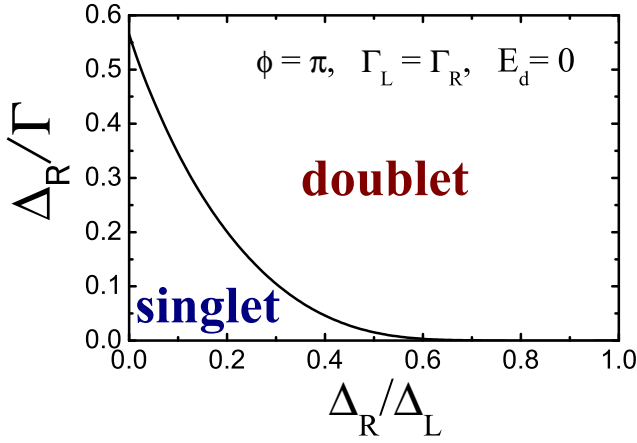


Fig. 1. Phase diagram of the ground state for $\phi = \pi$, $\Gamma_L = \Gamma_R$ ($\equiv \Gamma$), and $E_d = 0$. Here $|\Delta_L|$ is chosen to be $|\Delta_L| \geq |\Delta_R|$. An infinitesimal U lifts the 4-fold degeneracy caused by the zero mode to stabilize the singlet or doublet state depending on the value of $|\Delta_R|/|\Delta_L|$ and $1/\Gamma$. The results are obtained with the perturbation theory in Appendix D.

3. Bound state in the gap

The bound state appearing in the SC gap plays an important role on the ground-state properties of dilute magnetic alloys.¹⁻³ In the case of the quantum dots, the Josephson phase $\phi = \theta_R - \theta_L$ also changes the energy and wavefunction of the bound state,¹⁷ and it also affects the screening of the local moment. To make these features of the ϕ dependence of the bound state clear, we discuss briefly about the bound state in the noninteracting case [see also Appendix B].

The bound state can exist in the gap region $|\epsilon| < \min(|\Delta_L|, |\Delta_R|)$, and the eigenvalue is determined by the equation $\det \{G_{dd}^0(\epsilon)\}^{-1} = 0$. For noninteracting electrons the determinant can be written explicitly as,

$$\det \{G_{dd}^0(\epsilon)\}^{-1} = 2 [F_2(\epsilon^2) - F_1(\epsilon^2)] , \quad (21)$$

$$F_1(\epsilon^2) \equiv \frac{1}{2} [\Gamma_L^2 + \Gamma_R^2 + E_d^2 - \epsilon^2] , \quad (22)$$

$$F_2(\epsilon^2) \equiv \frac{\Gamma_L \epsilon^2}{\sqrt{|\Delta_L|^2 - \epsilon^2}} + \frac{\Gamma_R \epsilon^2}{\sqrt{|\Delta_R|^2 - \epsilon^2}} + \frac{\Gamma_L \Gamma_R (\epsilon^2 - |\Delta_L| |\Delta_R| \cos \phi)}{\sqrt{|\Delta_L|^2 - \epsilon^2} \sqrt{|\Delta_R|^2 - \epsilon^2}} . \quad (23)$$

Here $F_1(\epsilon^2)$ is a simple decreasing function of ϵ^2 , while the functional form of $F_2(\epsilon^2)$ depends on the parameters $|\Delta_L|$, $|\Delta_R|$ and ϕ . However, at $\epsilon = 0$, it is given simply by $F_2(0) = -\Gamma_L \Gamma_R \cos \phi$. Therefore $F_1(0) \geq F_2(0)$, and the equality holds for $\phi = \pi$, $\Gamma_L = \Gamma_R$ and $E_d = 0$. We consider this particular case in the following, and then discuss briefly the bound state for the models mentioned in §2.

3.1 Zero mode for $\phi = \pi$, $\Gamma_R = \Gamma_L$ and $E_d = 0$

We consider here the special case where the three conditions hold simultaneously; *i*) π -junction $\phi = \pi$, *ii*) equal coupling $\Gamma_L = \Gamma_R$ ($\equiv \Gamma$), and electron-hole sym-

metry $E_d = 0$. In this case $F_2(\epsilon^2)$ is a increasing function of ϵ^2 , and at $\epsilon = 0$ it coincides with $F_1(0)$, so that the bound state comes just on the Fermi energy $\epsilon = 0$.

Thus, the ground state has 4-fold degeneracy with respect to the occupation of the zero-energy bound state by the Bogoliubov quasiparticles [see also Appendix C]. The Coulomb interaction \mathcal{H}_d^U lifts the degeneracy. We have calculated the energy shift for an infinitesimal positive U using the perturbation theory, the outline of which is given in Appendix D. The ground state is a singlet for $\Gamma > \Gamma_{cr}$, while it is a doublet for $\Gamma < \Gamma_{cr}$. The critical value Γ_{cr} depends on the ratio $x \equiv |\Delta_R|/|\Delta_L|$ as shown in Fig. 1. In this figure the phase boundary is plotted in the x vs $1/\Gamma$ plane choosing $|\Delta_L|$ to be $|\Delta_L| \geq |\Delta_R|$, where the energy is scaled by $|\Delta_R|$. The critical value Γ_{cr} increases with x and diverges exponentially at $x = 1$, and thus for $|\Delta_L| = |\Delta_R|$ the ground state is a doublet independent of the value of Γ . This is because in this particular case the SC correlation penetrates from the left lead and that from the right cancel each other out to make the net SC correlation at the impurity site χ_d^0 to be zero. This example shows that the asymmetry in the two gaps $|\Delta_L| \neq |\Delta_R|$ affects the screening of the moment crucially when the other parameters are set to be highly symmetric. Note that in the perturbation theory an exchange integral (Fock term) of the form Eq. (12) shifts the bound state from the Fermi level and favors the singlet state, whereas a direct type contribution (Hartree term) favors the doublet state.

3.2 Bound state for Models I & II

When the absolute value of the two gaps are the same, $|\Delta_L| = |\Delta_R| \equiv \Delta$, Eq. (23) simplifies as

$$F_2(\epsilon^2) = \frac{(\Gamma_L + \Gamma_R) \epsilon^2}{\sqrt{\Delta^2 - \epsilon^2}} - \Gamma_L \Gamma_R + \frac{2 \Gamma_L \Gamma_R \Delta^2 \sin^2 \frac{\phi}{2}}{\Delta^2 - \epsilon^2} . \quad (24)$$

Since this is an increasing function of ϵ^2 which diverges positively at $\epsilon^2 \rightarrow \Delta^2$, the bound state exists for any finite Δ .

For the other model with the asymmetric gap $|\Delta_L| \gg |\Delta_R|$, the function $F_2(\epsilon^2)$ is given by

$$F_2(\epsilon^2) = \Gamma_R \frac{\epsilon^2 - \Delta_d |\Delta_R| \cos \phi}{\sqrt{|\Delta_R|^2 - \epsilon^2}} , \quad (25)$$

where $\Delta_d \equiv \Gamma_L$. In this case the behavior of $F_2(\epsilon^2)$ at $\epsilon^2 \rightarrow |\Delta_R|^2 - 0^+$ depends crucially on the sign of the numerator, and thus whether or not the bound state exists depends on the values of the parameters.

4. NRG approach

In the rest of this paper we discuss the ground state properties of the Anderson impurity in the limit of $|\Delta_L| \gg |\Delta_R|$, where one of the SC gaps is much larger than that of the others, based on the single-channel model given by Eq. (19). As mentioned in §2.2, this model contains essential aspects of both the Josephson and Kondo effects. Also, the reduction in the number of the channels gives us a practical advantage in the NRG calculations.

4.1 Method

Through a standard procedure of the logarithmic discretization,²³ the conduction band can be modelled by a linear chain with the complex pair potential $\Delta_R = |\Delta_R|e^{i\phi}$, and a sequence of the NRG Hamiltonian H_N is given by

$$H_N = \Lambda^{(N-1)/2} [\mathcal{H}_d^0 + \mathcal{H}_d^U + \mathcal{H}_d^{\text{SC}} + H_{dR} + H_R], \quad (26)$$

$$H_R = D \frac{1 + 1/\Lambda}{2} \times \sum_{n=0}^{N-1} \sum_{\sigma} \xi_n \Lambda^{-n/2} \left(f_{n+1\sigma}^{\dagger} f_{n\sigma} + f_{n\sigma}^{\dagger} f_{n+1\sigma} \right) + \sum_{n=0}^N \left(\Delta_R f_{n\uparrow}^{\dagger} f_{n\downarrow}^{\dagger} + \Delta_R^* f_{n\downarrow} f_{n\uparrow} \right), \quad (27)$$

$$H_{dR} = D \sum_{\sigma} \tilde{v}_R \left(f_{0\sigma}^{\dagger} d_{\sigma} + d_{\sigma}^{\dagger} f_{0\sigma} \right). \quad (28)$$

Here D is the half-width of the conduction band, and $f_{n\sigma}$ is an operator for electrons in the right lead. The hopping matrix elements ξ_n and \tilde{v}_R are defined by

$$\xi_n = \frac{1 - 1/\Lambda^{n+1}}{\sqrt{1 - 1/\Lambda^{2n+1}} \sqrt{1 - 1/\Lambda^{2n+3}}}, \quad (29)$$

$$\tilde{v}_R = \sqrt{\frac{2\Gamma_R A_{\Lambda}}{\pi D}}, \quad A_{\Lambda} = \frac{1}{2} \frac{1 + 1/\Lambda}{1 - 1/\Lambda} \log \Lambda, \quad (30)$$

where $A_{\Lambda} \rightarrow 1$, in the continuum limit $\Lambda \rightarrow 1$.^{23,24} The low-lying energy states of \mathcal{H}_{eff} can be deduced from that of $\Lambda^{-(N-1)/2} H_N$ for large N . In the presence of the complex SC gap H_N does not conserve the charge, and the total spin S is the only one quantum number that can be used for the block diagonalization. In the two special cases, $\phi = 0$ and π , the Hamiltonian H_N has an extra $U(1)$ symmetry corresponding to the x -th component of the axial charge $I_x = \sum_{n=-1}^N (-1)^n (f_{n\uparrow}^{\dagger} f_{n\downarrow}^{\dagger} + f_{n\downarrow} f_{n\uparrow})/2$ with $f_{-1\sigma}^{\dagger} \equiv d_{\sigma}^{\dagger}$,²³ and the SC lead can be transformed into a normal lead with a staggered potential.⁷

The ground-state average of the Josephson current can be obtained using the discretized version of Eq. (6),

$$\langle J \rangle_N = ie \tilde{v}_R D \sum_{\sigma} \left(\langle \Phi_N | f_{0\sigma}^{\dagger} d_{\sigma} | \Phi_N \rangle - \langle \Phi_N | d_{\sigma}^{\dagger} f_{0\sigma} | \Phi_N \rangle \right), \quad (31)$$

where $|\Phi_N\rangle$ is the ground state of H_N . The expectation value can be calculated successively for large N using the recursive relation among the matrix elements $\langle J \rangle_N$ and $\langle J \rangle_{N+1}$. We have carried out the calculations retaining the lowest 500 states and taking Λ and $|\Delta_R|$ to be $\Lambda = 2.0$ and $|\Delta_R|/D = 1.0 \times 10^{-5}$. In the following, we use $|\Delta_R|$ as the unit of the energy in most of the figures, since that is a typical energy scale for the superconductivity.

4.2 Results at half-filling

In this subsection we show the results obtained in the electron-hole symmetric case, $\epsilon_d = -U/2$. We first of all consider the ground state for $\Delta_d = 0$. Since the value

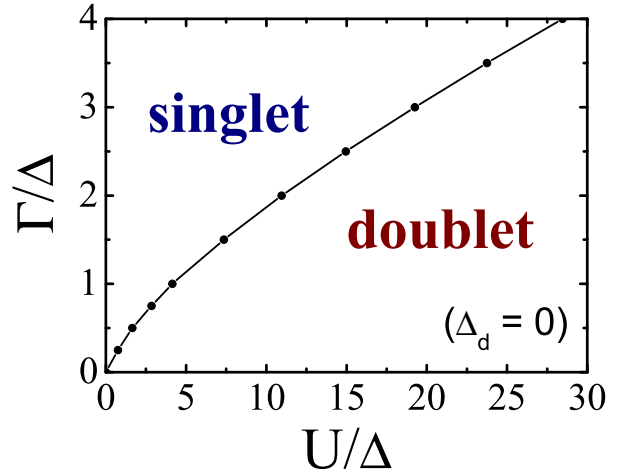


Fig. 2. Phase diagram of the ground state for the symmetric Anderson model $\epsilon_d = -U/2$ connected to the single SC lead of Δ , where the SC gap in the impurity site is taken to be $\Delta_d = 0$. The NRG calculations have been carried out for $\Lambda = 2.0$ and $\Delta/D = 1.0 \times 10^{-5}$.

of Δ_d is defined to be equal to Γ_L in the original two-channel model Eq. (1), the condition $\Delta_d = 0$ means that the left superconductor is disconnected completely from the impurity. In Fig. 2, the phase diagram of the ground state is shown as a function of $U/|\Delta_R|$ and $\Gamma_R/|\Delta_R|$. The ground state is a spin-singlet state for large Γ_R or small U , and it is a doublet for small Γ_R or large U . We note that this particular case, $\Delta_d = 0$, has been examined by Yoshioka and Ohashi,⁹ and the phase boundary is determined basically by a single parameter $T_K/|\Delta_R|$ in the Kondo regime. Nevertheless, for small U or the electron-hole asymmetric case, in which the contributions of the charge excitations still remain, the low-energy properties are characterized not only by the single parameter T_K , but the Wilson ratio R and the renormalized impurity level $\tilde{\epsilon}_d$ are necessary for a complete description.^{4,25} Therefore, in order to see an overall picture of the ground-state properties, the phase diagrams which are plotted as a function of the bare parameters, as Fig. 2, are convenient.

When the SC gap of the impurity $\Delta_d (\equiv \Gamma_L)$ becomes finite owing to the coupling with the left lead of $|\Delta_L| \rightarrow \infty$, the phase difference ϕ can be introduced at the interface of Δ_d and Δ_R . We now examine how ϕ affects the ground state in the equal-coupling case $\Gamma_L = \Gamma_R$. In Fig. 3 the phase diagram of the ground state is plotted as a function of U and Γ_R for several value of the phase difference $\phi = 0, \pi/2, 3\pi/4, \pi$. Here Δ_d is varied simultaneously with Γ_R keeping the relation $\Delta_d = \Gamma_R$. We see that ϕ tends to disturb the screening of the local moment and enlarges the doublet phase in the figure. The feature of the phase diagram at $\phi \neq \pi$ is similar to that for $\Delta_d = 0$ in Fig. 2. However, the feature is quite different for $\phi = \pi$. This is caused by the bound state lying just on the Fermi level at $U = 0$. An infinitesimal U lifts the degeneracy to stabilize the singlet state at $\Gamma_R > \Gamma_{\text{cr}}$, and doublet state at $\Gamma_R < \Gamma_{\text{cr}}$. In

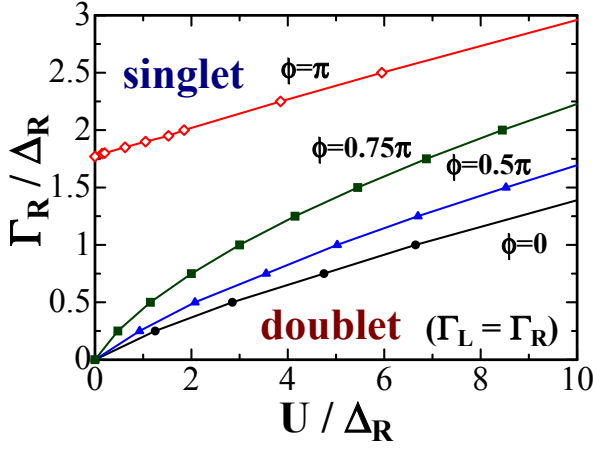


Fig. 3. Phase diagram of the ground state for the equal coupling $\Gamma_L = \Gamma_R$ at half-filling $\epsilon_d = -U/2$ is plotted for several values of the Josephson phase ϕ . Here $\Delta_d (\equiv \Gamma_L)$ is taken to be equal to Γ_R . For $\phi = \pi$ and $U = 0$, the phase boundary is given by $\Gamma_{cr} = 1.77064|\Delta_R|$. This special behavior at $\phi = \pi$ is caused by the zero mode, and an infinitesimal U stabilizes the singlet (doublet) ground state for $\Gamma_R > \Gamma_{cr}$ ($\Gamma_R < \Gamma_{cr}$).

the present model, $\Delta_L \rightarrow \infty$, the critical value is given by $\Gamma_{cr} = 1.77064|\Delta_R|$ as described in Appendix D. For this reason, in Fig. 3 the phase boundary for $\phi = \pi$ starts from the finite value, Γ_{cr} , in the y axis.

To see how the singlet or doublet ground states evolves in the successive NRG steps, in Fig. 4 the low-lying energy levels of $\Lambda^{-(N-1)/2}H_N$ is plotted as a function of N for (a) $U = |\Delta_R|$, and (b) $U = 9.0|\Delta_R|$. Here the factor $\Lambda^{-(N-1)/2}$ restores the original energy scale of \mathcal{H}_{eff} , and the ground-state energy is subtracted from the eigenvalue for the excited states. The parameters are taken to be $\phi = \pi$ and $\Gamma_R = 1.5|\Delta_R|$. Specifically, the SC gap in the impurity site is chosen to be $\Delta_d = |\Delta_R|$, so that the couplings are asymmetric $\Gamma_L \neq \Gamma_R$ in this parameter set. In the figure the eigenstates are labeled by the two quantum numbers $(I_x, 2S)$, where I_x is the U(1)-axial charge mentioned in the above and S is the total spin. The solid and open symbols correspond to the levels for even and odd N , respectively. For large N , the excitation energies converge to the fixed point values, and have no even-odd oscillatory dependence on N , which is a typical behavior seen in the presence of the energy gap.⁷ The ground state is a singlet for $N \gtrsim 32$ in (a), while it is a doublet in the case of (b). In the figures all the low-lying levels are shown for $E < |\Delta_R|$, but not all are shown for $E > |\Delta_R|$. The levels below the gap $|\Delta_R|$ can be classified according to the occupation of the bound state with the Bogoliubov quasiparticles, which can be inferred from the value of I_x because it is transformed into the usual charge by the Unitary transformation described in Ref. 7. In the case of (a), where U is relatively small, the first and second excited states lie in the gap region. The occupation of the bound state in the ground, first, and second excited states are supposed to be empty, single, and double, respectively. In contrast, in (b) the occupation of the bound state in the ground and first excited states are supposed to be single and empty, respectively.

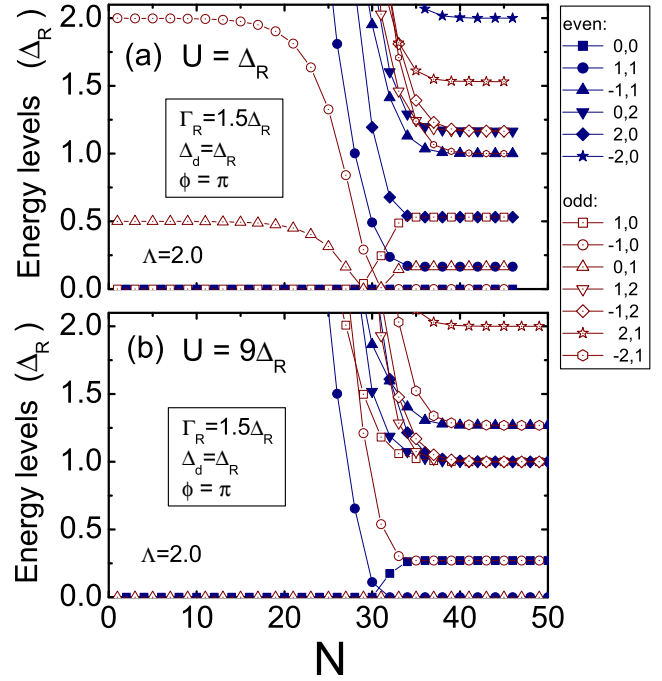


Fig. 4. Low-lying energy levels of $\Lambda^{-(N-1)/2}H_N$ as a function of N , where the energy is scaled by $|\Delta_R|$ and is measured from the ground-state energy at each N . The solid and open symbols are the levels for even and odd N , respectively. Only the lowest eigenvalue in each subspace labeled by the quantum numbers $(I_x, 2S)$ are shown, where I_x is the U(1)-axial charge and S is the total spin. The parameters are taken to be $\phi = \pi$, $\Delta_d = |\Delta_R|$, $\Gamma_R = 1.5|\Delta_R|$, $\epsilon_d = -U/2$, and $\Lambda = 2.0$. At large N , the levels approach to the fixed point values showing no even-odd dependence on N . For $N \gtrsim 32$, the ground state is a singlet in (a) $U = |\Delta_R|$, while it is a doublet in (b) $U = 9|\Delta_R|$.

The doubly occupied state could not stay below the gap in (b) because of large U .

The eigenvalues depend on the phase difference ϕ , and particularly the fixed-point energy at large N determines the low-energy properties. In Fig. 5, the fixed-point value of the lowest excitation energy $E_{S=0} - E_{S=1/2}$ is plotted as a function of U for several values of ϕ , where $E_{S=0}$ and $E_{S=1/2}$ are the lowest eigenvalues of $\Lambda^{-(N-1)/2}H_N$ in the singlet and doublet subspace, respectively. The parameters are chosen to be $\Gamma_R = 3.77697|\Delta_R|$, and $\Delta_d = \Delta_R$. For $U < U_C$ with $U_C \simeq 25|\Delta_R|$, the ground state is a singlet, and the excitation energy depends visibly on ϕ . The energy separation between the two states decreases with increasing ϕ , and it means that ϕ tends to destabilize the singlet ground state. On the other hand the ground state is a doublet for $U > U_C$, and the ϕ dependence of the excitation energy is very weak. This seems to be caused by the fact that the local moment, which remains in the doublet ground state, makes the SC correlation length small, and the phase coherence between the dot and SC lead becomes weak. In the singlet state, however, the phase coherence is preserved, and thus the excitation energy depends sensitively on ϕ . We can also see in Fig. 5 that the critical value U_C decreases with increasing ϕ to reduce the area of the singlet ground state in the phase diagram.

For asymmetric couplings $\Gamma_R \neq \Gamma_L$, the phase diagram

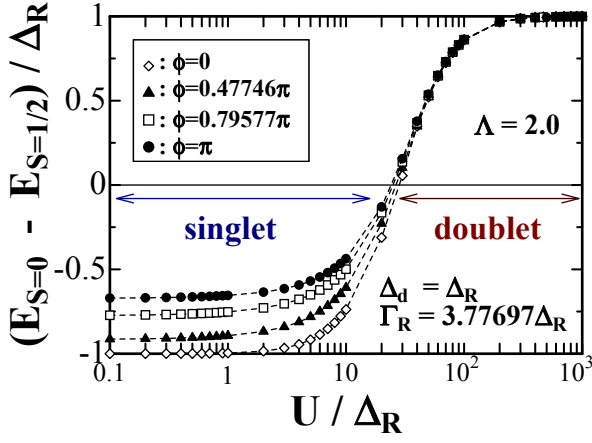


Fig. 5. The fixed point value of the lowest excitation energy of $\Lambda^{-(N-1)/2}H_N$ at large N as a function of U . Here $E_{S=0}$ and $E_{S=1/2}$ are the eigenvalue of the lowest singlet and doublet states, respectively. Therefore, the ground state is a singlet (doublet) for negative (positive) $E_{S=0} - E_{S=1/2}$. The parameters are taken to be $\Delta_d = |\Delta_R|$, $\Gamma_R = 3.77697|\Delta_R|$, $\epsilon_d = -U/2$, and $\Lambda = 2.0$.

of the ground state has some different features from that of the equal coupling case seen in Fig. 3. Two typical examples for the asymmetric coupling are shown in Fig. 6 for several values of ϕ . Here the value of Δ_d is fixed to be (a) $|\Delta_R|$ and (b) $2|\Delta_R|$ independent of the coupling Γ_R . In each of the figures (a) and (b), all the lines start from the same point on the horizontal line, the position of which is given by $U = 2\Delta_d$ from the atomic-limit solution at $\Gamma_R = 0$. A re-entrant behavior seen for $\phi \simeq \pi$ is caused by the bound state lying near the Fermi level. The phase boundary for $\phi = \pi$ crosses the vertical axis at $\Gamma_R = \Delta_d$, at which the couplings becomes equal $\Gamma_L = \Gamma_R$ and the bound state comes just on the Fermi level. An infinitesimal U lifts the 4-fold degeneracy of the ground state as shown in Fig. 1, and specifically in the present case, $\Delta_L \rightarrow \infty$, the critical value is given by $\Gamma_{cr} = 1.77064|\Delta_R|$ (see Appendix D). Thus the examples (a) and (b) represent typical cases of $\Delta_d < \Gamma_{cr}$ and $\Delta_d > \Gamma_{cr}$, respectively. In (b), the ground state is a singlet on the dotted horizontal line starting from $\Gamma_R = \Delta_d$, and the transition to the doublet state occurs discontinuously at finite U at the end of the dotted line. These examples show that the quantum phase transition can be driven by ϕ if the other parameters are in the region surrounded by the lines for $\phi = 0$ and that for $\phi = \pi$.

We next study how the Coulomb interaction affects the Josephson current. To this end, we start with noninteracting case. In Fig. 7 the Josephson current for $U = 0$, which is obtained from Eq. (13), is plotted as a function of ϕ for several values of Γ_R . Here the parameters are taken to be $\Delta_d = |\Delta_R|$, and thus at $\Gamma_R = |\Delta_R|$ the two couplings of the original model become equal $\Gamma_R = \Gamma_L$ since $\Delta_d \equiv \Gamma_L$. When the two couplings are close $\Gamma_R \simeq \Gamma_L$, the amplitude of the current becomes large, and the shape of the ϕ dependence deviates from a simple sinusoidal form. In the figure the dotted line is the result for $\Gamma_R = \Gamma_L$, and it shows a discontinuous jump at $\phi = \pm\pi$. This singularity is caused by the bound state at Fermi level. The NRG results of the Josephson

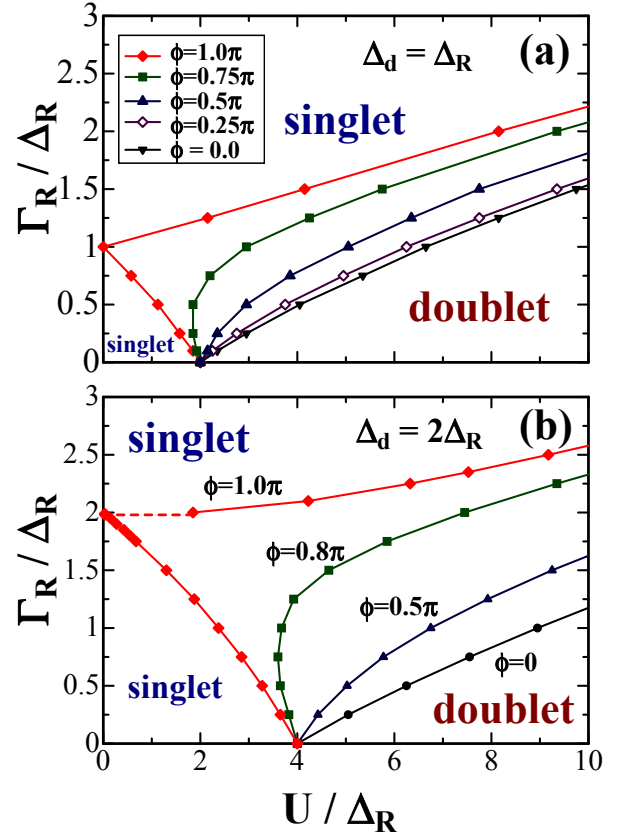


Fig. 6. Phase diagrams of the ground state in the electron-hole symmetric case $\epsilon_d = -U/2$. Here the impurity SC gap is taken to be (a) $\Delta_d = |\Delta_R|$, and (b) $\Delta_d = 2|\Delta_R|$. At $\Gamma_R = 0$, the phase boundary is given by $U = 2\Delta_d$ from the atomic-limit solution. For $\phi = \pi$, the bound state comes just on the Fermi level when $U = 0$ and $\Gamma_R = \Delta_d$ ($\equiv \Gamma_L$). In the case of (b), this happens in the region of $\Gamma_R > \Gamma_{cr} = 1.77064|\Delta_R|$, and on the dotted horizontal line the ground state is a singlet.

current are shown in Fig. 8 for several values of U , where the parameters are taken to be $\Gamma_R = 3.77697|\Delta_R|$, and $\Delta_d = |\Delta_R|$. In this figure the results are plotted only for $0 \leq \phi \leq \pi$. The feature of the current at negative ϕ can be seen by rotating the figure around the origin, since the current is an odd function of ϕ with the period 2π . For small U , the ground state is a singlet for the whole range of ϕ as seen in the results for $U \lesssim 20|\Delta_R|$, and in these cases the amplitude of the current decreases with increasing U . We see for $U = 25|\Delta_R|$ that the phase transition occurs at $\phi \simeq 0.76\pi$. Then in the doublet state the current flows in the opposite direction from that in the singlet state. This change is caused by the spin-flip tunneling through the unscreened local moment.^{13,14} Therefore, the Josephson current can be used to detect the quantum phase transition.

In quantum dots the coupling to the leads is a tunable parameter. We have plotted the current as a function of ϕ in Fig. 9 for several values of Γ_R taking U to be (a) $5.0|\Delta_R|$ and (b) $15.0|\Delta_R|$. Here the gap is chosen to be $\Delta_d = |\Delta_R|$. Both in (a) and (b), the phase transition from the singlet state to doublet state occurs when Γ_R decreases. It can be explained from the fact that the correlation effects are enhanced for small Γ_R . However, the

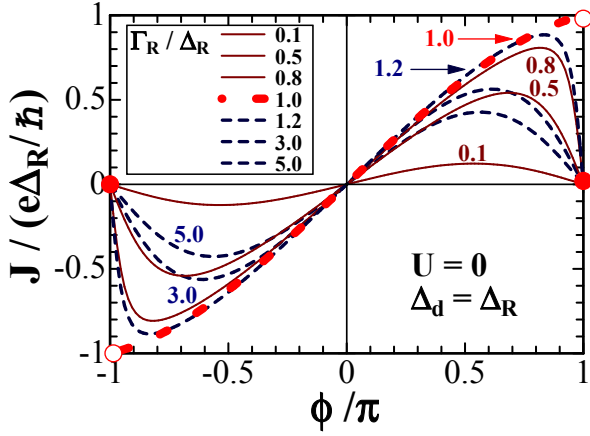


Fig. 7. The Josephson current for $U = 0$ and $E_d = 0$ as a function of ϕ . The currents are calculated for several values of Γ_R from Eq. (13). Here $\Delta_d (\equiv \Gamma_L)$ is taken to be $\Delta_d = |\Delta_R|$, so that Γ_R becomes equal to Γ_L for $\Gamma_R/|\Delta_R| = 1.0$, where the current for $\phi = \pm\pi$ jumps discontinuously.

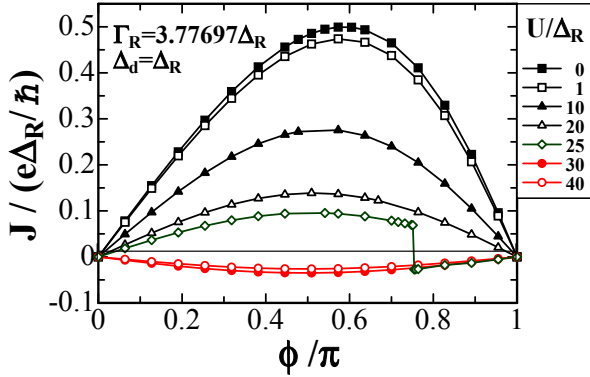


Fig. 8. The Josephson current as a function of ϕ for various values of U . Here the parameters are taken to be $\Gamma_R = 3.77697\Delta_R$, $\Delta_d = \Delta_R$, and $\epsilon_d = -U/2$. The ground state is a singlet for $U \lesssim 20\Delta_R$, while it is a doublet for $U \gtrsim 30\Delta_R$. For $U = 25\Delta_R$, the quantum phase transition to the doublet ground state occurs at $\phi \simeq 0.76\pi$, and the direction of the current changes due to the spin-flip tunneling.¹³ Note that the current for negative ϕ is symmetric around the origin as that in Fig. 7, since the current is an odd function of ϕ with the period 2π .

amplitude of the current depends on another factor. In Fig. 9 (a), the amplitude becomes large when the value of Γ_R approaches $\Gamma_L (\equiv \Delta_d)$. In this case, the matching condition at the interface is the dominant factor that determines the amplitude of the current. On the other hand, the amplitude decreases with Γ_R in Fig. 9 (b). In this case, the ground state is a doublet when Γ_R becomes equal to Γ_L , and thus in the singlet state at $\Gamma_R > \Gamma_L$ the strong electron correlation dominates the matching condition to make the amplitude of the current small.

4.3 Results away from half-filling

So far, we have discussed the results at half-filling $\epsilon_d = -U/2$, where the impurity site is singly occupied in average. In that case, the magnetic correlations are enhanced, while the charge excitations are suppressed. Therefore, when the system goes away from half-filling,

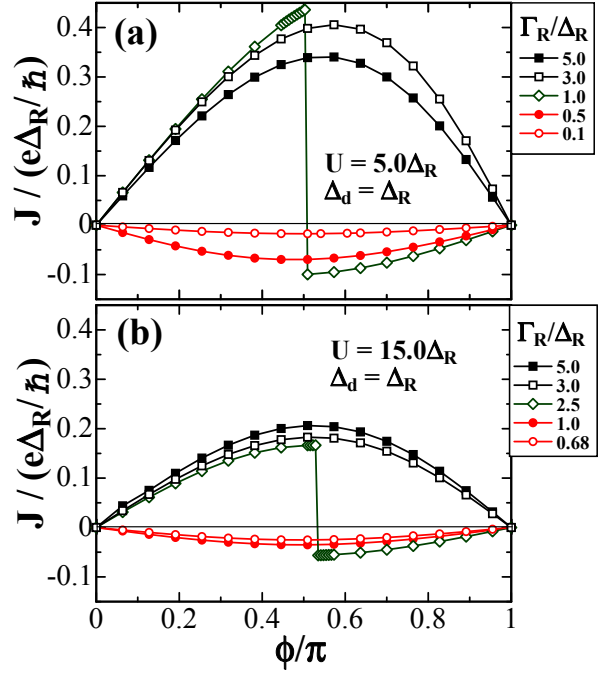


Fig. 9. The Josephson current as a function of ϕ for various values of Γ_R : the onsite Coulomb repulsion is taken to be (a) $U = 5.0|\Delta_R|$ and (b) $U = 15.0|\Delta_R|$. Other parameters are $\Delta_d = |\Delta_R|$, and $\epsilon_d = -U/2$.

the magnetic doublet ground state should be destabilized. In quantum dots the impurity potential ϵ_d is the parameter that can be controlled by the gate voltages. We show in the following the NRG results for the ground-state properties in the electron-hole asymmetric case.

In Fig. 10, one example of the phase diagram is plotted as a function of U and Γ_R , where $\epsilon_d = -2.5|\Delta_R|$ and $\Delta_d = |\Delta_R|$. The model has the electron-hole symmetry at $U = 5.0|\Delta_R|$ and the results coincide with that at the same U in Fig. 6(a). As expected, the region where the doublet state stabilized becomes narrow away from half-filling. Particularly the re-entrant region of the doublet state, which is seen at half-filling, almost vanishes in the case of Fig. 10. At $\Gamma_R = 0$, all the lines for different ϕ start from $U_a = (\epsilon_d^2 + \Delta_d^2)/(-\epsilon_d)$, where the level crossing occurs in the atomic limit. Then, for large U , the boundaries become flat. We next consider the ϵ_d dependence of the ground state. In the following two figures, the phase diagrams are plotted in a Γ_R vs ϵ_d plane for two different values of U : it is chosen to be $U = 5.0|\Delta_R|$ and $U = 1.0|\Delta_R|$ in Figs. 11 and 12, respectively. Here the impurity SC gaps is taken to be $\Delta_d = |\Delta_R|$. The figure 11 is an example of the phase diagram for large U , where the impurity is half-filled at $\epsilon_d = -2.5|\Delta_R|$, and the doublet phase vanishes when ϵ_d or $\epsilon_d + U$ approaches the Fermi level at $\mu = 0$. The doublet region becomes wider with increasing ϕ , and this tendency is maximized at $\phi = \pi$. For small U , the re-entrant doublet region appears as an *island* in the phase diagram Fig. 12, where the line for $\phi = \pi$ is shown. The magnetic doublet state is most stable at half-filling $\epsilon_d = -0.5|\Delta_R|$. In this re-entrant region, the bound state lies close to the Fermi level.

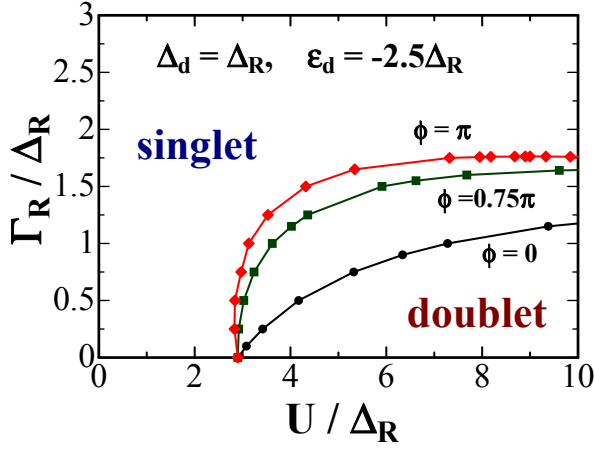


Fig. 10. Phase diagrams of the ground state away from half-filling for several values of the phase difference ϕ , where $\epsilon_d = -2.5|\Delta_R|$ and $\Delta_d = |\Delta_R|$.

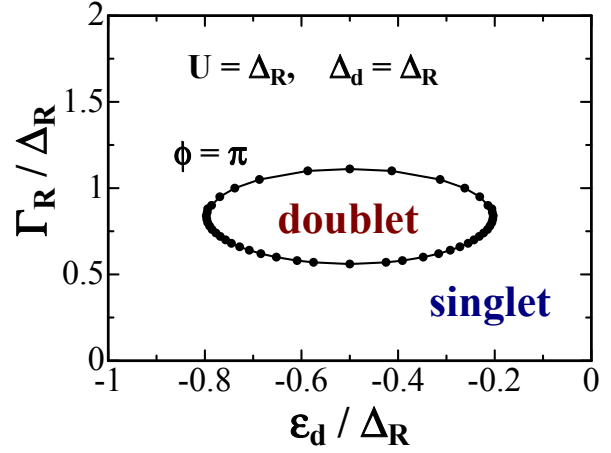


Fig. 12. Phase diagrams of the ground state as a function of ϵ_d and Γ_R , where $\phi = \pi$, $\Delta_d = |\Delta_R|$ and $U = 1.0|\Delta_R|$. Note that the scale of the horizontal axis is different from that of Fig. 11.

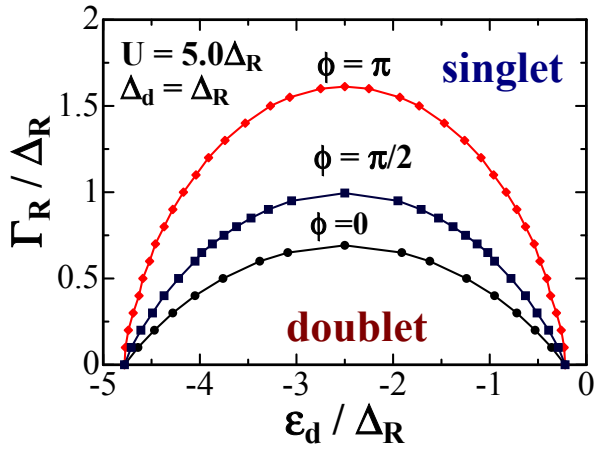


Fig. 11. Phase diagrams of the ground state as a function of ϵ_d and Γ_R , where $\Delta_d = |\Delta_R|$ and $U = 5.0|\Delta_R|$.

We have also calculated the Josephson current and the average number of electrons in the impurity site $\langle n_d \rangle$. In Fig. 13, the results are plotted as a function of ϵ_d for (a) $\Gamma_R = 1.7|\Delta_R|$ and (b) $\Gamma_R = 0.3|\Delta_R|$. The parameters are taken to be $\phi = 0.5\pi$, $\Delta_d = |\Delta_R|$, and $U = 5.0|\Delta_R|$; the ground state for these parameters are shown in Fig. 11. In the case of (a), the ground state is a singlet independent of ϵ_d . The current shows a maximum at half-filling $\epsilon_d = -2.5|\Delta_R|$, and $\langle n_d \rangle$ decreases monotonically with increasing ϵ_d . On the other hand, in the case of (b), the quantum phase transition occurs near half-filling, where the doublet state is stabilized. The expectation values show the singular behavior at the critical point, and particularly the Josephson current becomes small and changes the direction.

5. Summary

In summary, we have studied the ground-state properties of a model for the quantum dot embedded in the Josephson junction making use of the NRG method. To carry out precise calculations in a wide parameter range, we have introduced a simplified single-channel model

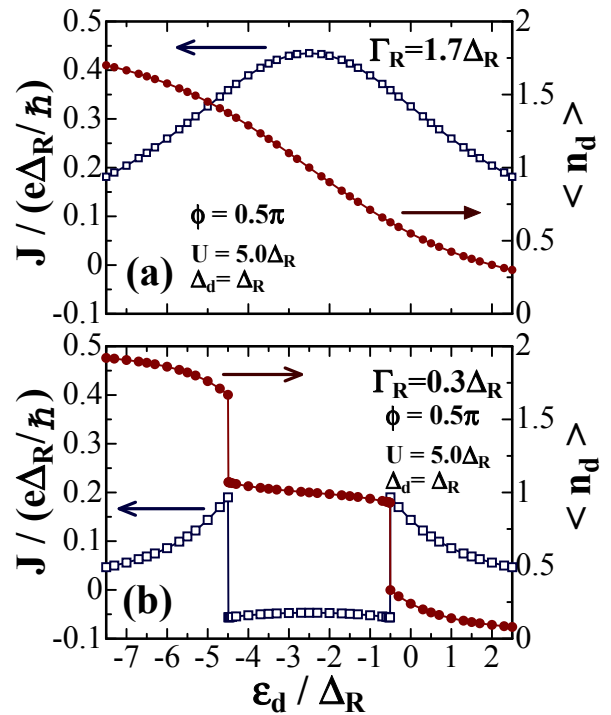


Fig. 13. The Josephson current and the number of the electrons in the impurity $\langle n_d \rangle$ as a function of ϵ_d for (a) $\Gamma_R = 1.7|\Delta_R|$ and (b) $\Gamma_R = 0.3|\Delta_R|$. The parameters are taken to be $\phi = 0.5\pi$, $\Delta_d = |\Delta_R|$, and $U = 5.0|\Delta_R|$. The ground state is a singlet in the case (a), while in (b) the quantum transition occurs and the doublet state is stabilized around half-filling.

that has an extra superconducting gap Δ_d at the impurity site. This model captures the essence of the Josephson and Kondo physics, and can be derived from the two-channel model when one of the bulk SC gaps is much larger than the others $|\Delta_L| \gg |\Delta_R|$. This kind of asymmetry in the Josephson couplings causes the nontrivial changes in the superconducting proximity effects on the impurity site, and it affects the low-energy spin dynamics of the quantum impurity.

The numerical results for the simplified model show

that the Josephson phase tends to disturb the conduction electron screening of the local moment, and destabilizes the paramagnetic singlet ground state to drive a quantum phase transition to the magnetic doublet ground state. At the transition point, the direction of the Josephson current changes discontinuously due to the spin-flip tunneling. Specifically, when the Josephson phase is $\phi \simeq \pi$ and the other parameters are set so that the conductance in a normal limit $\Delta_R, \Delta_L \rightarrow 0$ is close to the unitary limit value, the bound state comes near the Fermi level. This zero mode causes a re-entrant magnetic phase transition for the asymmetric Josephson couplings.

It is known for the Anderson impurity in normal metals that the magnetic transition described by the mean-field theory is an artifact due to the approximation, i.e., quantum fluctuations stabilize the singlet ground state. In the superconducting case, however, the gap changes the structures of the low-energy excitations, and makes the occurrence of the quantum phase transition possible, the phase diagrams for which are provided in the present paper. The asymmetries in the Josephson couplings and the phase difference of the gaps add interesting varieties in the ground-state properties of the Kondo system through the changes in the bound state.

Acknowledgements

We are grateful to O. Sakai and Y. Shimizu for valuable discussions. One of us (AO) wishes to acknowledge a support by the Grant-in-Aid for Scientific Research from JSPS. ACH wishes to thank the EPSRC(Grant GR/S18571/01) for financial support. Numerical computation was partly performed at computation center of Nagoya University and at Yukawa Institute Computer Facility.

Appendix A: Functional method

The impurity part of the partition function can be expressed using the path integral formulation as

$$Z_{\text{eff}} = \int \mathcal{D}\eta^\dagger \mathcal{D}\eta e^{-S_{\text{eff}}}, \quad (\text{A}\cdot 1)$$

$$S_{\text{eff}} = \int_0^\beta \int_0^\beta d\tau d\tau' \begin{bmatrix} \eta_\uparrow^\dagger(\tau) \\ \eta_\downarrow^\dagger(\tau) \end{bmatrix} \mathbf{K}_{dd}^0(\tau, \tau') \begin{bmatrix} \eta_\uparrow(\tau') \\ \eta_\downarrow(\tau') \end{bmatrix} - \frac{U}{2} \int_0^\beta d\tau \left(\sum_\sigma \eta_\sigma^\dagger(\tau) \eta_\sigma(\tau) - 1 \right)^2, \quad (\text{A}\cdot 2)$$

$$\mathbf{K}_{dd}^0(\tau, \tau') = \frac{1}{\beta} \sum_{\omega_n} \{ \mathbf{G}_{dd}^0(i\omega_n) \}^{-1} e^{-i\omega_n(\tau - \tau')}, \quad (\text{A}\cdot 3)$$

where $\eta_\sigma(\tau)$ is a Grassmann number. The information about the conduction electrons enters into S_{eff} through the noninteracting Green's function $\mathbf{G}_{dd}^0(i\omega_n)$. Thus, if the different Hamiltonians give the same $\mathbf{G}_{dd}^0(i\omega_n)$, they also describe the same local properties around the impurity.²⁶

Appendix B: Bogoliubov-de Gennes representation

We provide here the expression of the Green's function in terms of the Bogoliubov quasiparticles, which will be used in Appendix D to carry out the perturbative calculations. The noninteracting Hamiltonian, $\mathcal{H}^0 \equiv \mathcal{H}_d^0 + \sum_{\lambda=L,R} (\mathcal{H}_\lambda + \mathcal{H}_{d\lambda}^T)$, can be diagonalized using the Bogoliubov operator $\gamma_{n\sigma}$;

$$\mathcal{H}_0 = E_b \sum_\sigma \gamma_{0\sigma}^\dagger \gamma_{0\sigma} + \sum_\sigma \sum_{n>0} E_n \gamma_{n\sigma}^\dagger \gamma_{n\sigma} + \text{const.} \quad (\text{B}\cdot 1)$$

Here the label $n = 0$ is assigned to the bound state in the gap, and that for $n > 0$ corresponds to the excitations in the continuum $E_n \geq \min(|\Delta_L|, |\Delta_R|)$. Then the impurity Green's function can be written as,

$$\mathbf{G}_{dd}^0(i\omega_l) = \mathbf{U}_{d0} \frac{i\omega_l \mathbf{1} + E_b \boldsymbol{\tau}_3}{-\omega_l^2 - E_b^2} \mathbf{U}_{d0}^\dagger + \sum_{n>0} \mathbf{U}_{dn} \frac{i\omega_l \mathbf{1} + E_n \boldsymbol{\tau}_3}{-\omega_l^2 - E_n^2} \mathbf{U}_{dn}^\dagger. \quad (\text{B}\cdot 2)$$

Here, \mathbf{U}_{dn} is the matrix defined by the Unitary transformation

$$\begin{bmatrix} d_\uparrow \\ d_\downarrow \end{bmatrix} = \mathbf{U}_{d0} \begin{bmatrix} \gamma_{0\uparrow} \\ \gamma_{0\downarrow} \end{bmatrix} + \sum_{n>0} \mathbf{U}_{dn} \begin{bmatrix} \gamma_{n\uparrow} \\ \gamma_{n\downarrow} \end{bmatrix}, \quad (\text{B}\cdot 3)$$

$$\mathbf{U}_{dn} = \begin{bmatrix} u_{dn} & -v_{dn}^* \\ v_{dn} & u_{dn}^* \end{bmatrix}, \quad (\text{B}\cdot 4)$$

and it has a property $\mathbf{U}_{dn} \mathbf{U}_{dn}^\dagger = (|u_{dn}|^2 + |v_{dn}|^2) \mathbf{1}$. With these quasiparticle states, the SC correlation for noninteracting electrons $\chi_d^0 = \langle d_\downarrow d_\uparrow \rangle^0$ can be expressed as

$$\chi_d^0 = -u_{d0} v_{d0}^* \{1 - 2f(E_b)\} - \sum_{n>0} u_{dn} v_{dn}^* \{1 - 2f(E_n)\}. \quad (\text{B}\cdot 5)$$

Note that the first term in the right-hand side, which corresponds to the contributions of the bound state, vanishes if the bound state appears at the Fermi energy $E_b = 0$.

Appendix C: Correlation functions for the zero mode $E_b = 0$

As mentioned in §3, the bound state appears just on the Fermi level when $\phi = \pi$, $\Gamma_R = \Gamma_L$ ($\equiv \Gamma$), and $E_d = 0$. Around the pole at $E_b = 0$, the Green's function can be written in the form

$$\mathbf{G}_{dd}^0(\epsilon) \simeq \frac{a}{\epsilon + i0^+} \mathbf{1}, \quad (\text{C}\cdot 1)$$

$$a = \frac{1}{1 + \frac{\Gamma}{|\Delta_L|} + \frac{\Gamma}{|\Delta_R|}}. \quad (\text{C}\cdot 2)$$

The spectral weight at the impurity site, a , decreases with increasing Γ because the bound-state wavefunction penetrates deep inside the leads for large Γ . Alternatively, the Green's function can be expressed using Eq.

(B·2) as

$$\mathbf{G}_{dd}^0(\epsilon) \simeq \frac{|u_{d0}|^2 + |v_{d0}|^2}{\epsilon + i0^+} \mathbf{1}. \quad (\text{C} \cdot 3)$$

Therefore comparing Eqs. (C·2) and (C·3), we have $a = |u_{d0}|^2 + |v_{d0}|^2$. Furthermore, it is concluded that $|u_{d0}|^2 = |v_{d0}|^2 = a/2$ because of the electron-hole symmetry. Also, u_{d0} and v_{d0} are essentially real at $\phi = \pi$.

In the presence of the zero mode the expression of the SC correlation, Eq. (12), can be rewritten in the form

$$\begin{aligned} \chi_d^0 = & \frac{1}{\beta} \sum_{\omega_n} \frac{\Gamma \omega_n^2}{\det \{ \mathbf{G}_{dd}^0(i\omega_n) \}^{-1}} \frac{|\Delta_L|^2 - |\Delta_R|^2}{(\omega_n^2 + |\Delta_L|^2)(\omega_n^2 + |\Delta_R|^2)} \\ & \times \left[\frac{|\Delta_L|}{\sqrt{\omega_n^2 + |\Delta_L|^2}} + \frac{|\Delta_R|}{\sqrt{\omega_n^2 + |\Delta_R|^2}} \right]^{-1}. \end{aligned} \quad (\text{C} \cdot 4)$$

This expression clearly shows that χ_d^0 vanishes for $|\Delta_L| = |\Delta_R|$. Note that the behavior of the determinant near the bound state is deduced from Eq. (C·2) as $\det \{ \mathbf{G}_{dd}^0(i\omega_n) \}^{-1} \simeq -\omega_n^2/a^2$. In Eq. (C·4) this ω_n^2 dependence is canceled out by that in the numerator.

Appendix D: Perturbation theory for the zero mode

In the presence of the zero mode, i.e., for $\phi = \pi$, $\Gamma_L = \Gamma_R (\equiv \Gamma)$, and $E_d = 0$, the following four states are degenerate;

$$|\text{I}\rangle = |\tilde{0}\rangle, \quad (\text{D} \cdot 1)$$

$$|\text{II}\rangle = \gamma_{0\uparrow}^\dagger |\tilde{0}\rangle, \quad (\text{D} \cdot 2)$$

$$|\text{III}\rangle = \gamma_{0\downarrow}^\dagger |\tilde{0}\rangle, \quad (\text{D} \cdot 3)$$

$$|\text{IV}\rangle = \gamma_{0\uparrow}^\dagger \gamma_{0\downarrow}^\dagger |\tilde{0}\rangle. \quad (\text{D} \cdot 4)$$

Here $|\tilde{0}\rangle$ is the vacuum state with respect to the Bogoliubov particles $\gamma_{n\sigma}|\tilde{0}\rangle = 0$. An infinitesimal repulsion $\mathcal{H}_d^U = (U/2)(n_d - 1)^2$ lifts the degeneracy of the ground state. We have calculated the matrix elements $\langle \alpha | \mathcal{H}_d^U | \alpha' \rangle$ in this subspace making use of Eq. (B·3) and the equations provided in Appendix C. We found that the off-diagonal elements are zero

$$\langle \alpha | \mathcal{H}_d^U | \alpha' \rangle = 0, \quad \text{for } \alpha \neq \alpha', \quad (\text{D} \cdot 5)$$

and the energy shift is determined simply by the diagonal elements

$$\langle \text{I} | \mathcal{H}_d^U | \text{I} \rangle - \langle \text{II} | \mathcal{H}_d^U | \text{II} \rangle = \frac{U}{2} [a^2 - 2a\chi_d^0 \text{sgn}(u_{d0}v_{d0})], \quad (\text{D} \cdot 6)$$

$$\langle \text{IV} | \mathcal{H}_d^U | \text{IV} \rangle - \langle \text{II} | \mathcal{H}_d^U | \text{II} \rangle = \frac{U}{2} [a^2 + 2a\chi_d^0 \text{sgn}(u_{d0}v_{d0})]. \quad (\text{D} \cdot 7)$$

Note that $E_{S=1/2} \equiv \langle \text{II} | \mathcal{H}_d^U | \text{II} \rangle = \langle \text{III} | \mathcal{H}_d^U | \text{III} \rangle$ is the energy shift for the doublet states. Consequently, the energy difference between the doublet and the lowest singlet

states is given by

$$E_{S=0} - E_{S=1/2} = \frac{U}{2} [a^2 - 2a|\chi_d^0|]. \quad (\text{D} \cdot 8)$$

Thus the level crossing occurs at $a - 2|\chi_d^0| = 0$, where χ_d^0 is given by Eq. (C·4), and this equation determines the phase boundary between the doublet and singlet states. The results are shown in Fig. 1 as a function of the ratio $x \equiv |\Delta_R|/|\Delta_L|$. At $x = 0$, i.e., in the limit of $|\Delta_L| \rightarrow \infty$, Eq. (C·4) simplifies for $T = 0$ as

$$\begin{aligned} \chi_d^0 = & - \int_{-\infty}^{\infty} \frac{d\omega}{2\pi} \Gamma \\ & \times \left[\left(\sqrt{\omega^2 + |\Delta_R|^2} + 2\Gamma \right) \left(\sqrt{\omega^2 + |\Delta_R|^2} + |\Delta_R| \right) \right. \\ & \left. + 2\Gamma^2 \right]^{-1}, \end{aligned} \quad (\text{D} \cdot 9)$$

and the critical value of Γ is given by $\Gamma_{\text{cr}}/|\Delta_R| = 1.77064 \dots$. In the opposite limit at $x = 1 - 0^+$, i.e., for $|\Delta_L| = |\Delta_R|$, the critical value diverges exponentially as $\Gamma_{\text{cr}}/|\Delta_R| \simeq 4e^{[\pi/(1-x)+1]}$, so that the doublet ground state is stabilized for any values of Γ .

- 1) T. Soda, T. Matsuura, and Y. Nagaoka: Prog. Theor. Phys. **38** (1967) 551.
- 2) T. Matsuura: Prog. Theor. Phys. **57** (1977) 1823.
- 3) Müller-Hartman and J. Zittartz: Z. Phys. **234** (1970) 58.
- 4) A. C. Hewson: *The Kondo Problem to Heavy Fermions* (Cambridge University Press, Cambridge, 1993).
- 5) P. W. Anderson: Phys. Rev. **124** (1961) 41.
- 6) M. Jarrell, D. S. Sivia and B. Patton, Phys. Rev. B **42** (1990) 4804.
- 7) K. Satori, H. Shiba, O. Sakai and Y. Shimizu: J. Phys. Soc. Jpn. **61** (1992) 3239.
- 8) O. Sakai, Y. Shimizu, H. Shiba, and K. Satori: J. Phys. Soc. Jpn. **62** (1993) 3181.
- 9) T. Yoshioka and Y. Ohashi: J. Phys. Soc. Jpn. **69** (2000) 1812.
- 10) M. Matsumoto and M. Koga: J. Phys. Soc. Jpn. **70** (2001) 2860.
- 11) L. I. Glazman and K. A. Matveev: Pis'ma Zh. Eksp. Teor. Fiz. **49** (1989) 570 [JETP Lett. **49** (1989) 659].
- 12) C. W. J. Beenakker: in *Transport Phenomena in Mesoscopic Systems*, edited by H. Fukuyama and T. Ando (Springer-Verlag, Berlin, 1992).
- 13) I. O. Kulik: Soviet Physics JETP **22** (1966) 841.
- 14) H. Shiba and T. Soda: Prog. Theor. Phys. **41** (1969) 25.
- 15) B. I. Spivak and S. A. Kivelson: Phys. Rev. B **43** (1991) 3740.
- 16) S. Ishizaka, J. Sone and T. Ando: Phys. Rev. B **52** (1995) 8358.
- 17) A. A. Clerk and V. Ambegaokar: Phys. Rev. B **61** (2000) 9109.
- 18) A. V. Rozhkov and D. P. Arovas: Phys. Rev. Lett. **82** (1999) 2788.
- 19) Y. Avishai, A. Golub and A. D. Zaikin: Phys. Rev. B **67** (2003) 041301.
- 20) E. Vecino, A. Martín-Rodero, and A. Levy Yeyati: Phys. Rev. B **68** (2003) 035105.
- 21) K. Kusakabe, Y. Tanaka and Y. Tanuma: Physica E, **18** (2003) 50.
- 22) M.-S. Choi, M. Lee, K. Kang, and W. Belzig: cond-mat/031227.
- 23) H. R. Krishna-murth, J. W. Wilkins: and K. G. Wilson, Phys. Rev. B **21** (1980) 1003.
- 24) O. Sakai, Y. Shimizu, and T. Kasuya: Prog. Theor. Phys. Suppl. **108** (1992) 73.
- 25) A. C. Hewson: J. Phys.: Condens. Matter **13** (2001) 10011.
- 26) A. Oguri, J. Phys. Soc. Jpn. **71** (2002) 2696.